



## Sabino Matarrese

- Dipartimento di Fisica e Astronomia “Galileo Galilei”  
Università degli Studi di Padova, Italy
- INFN Sezione di Padova
- INAF Osservatorio Astronomico di Padova
- GSSI L’Aquila, Italy

# Cosmological Perturbation Theory and Primordial Gravitational Waves

*SIGRAV International School 2020 Gravity:  
General Relativity and beyond. Astrophysics,  
Cosmology and Gravitational Waves*

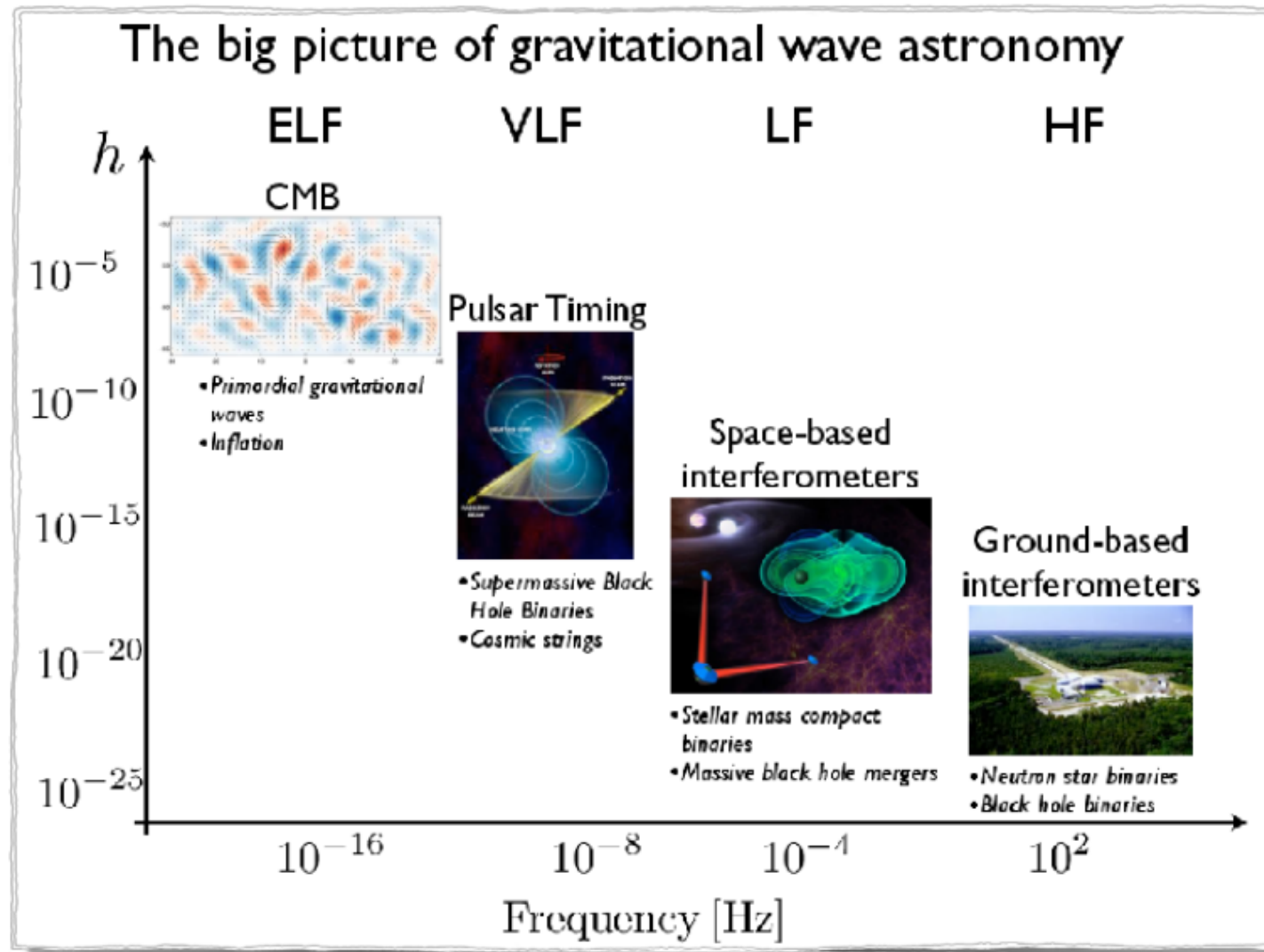
Vietri sul Mare 3-7 February 2020





- Cosmological Perturbation Theory. Gauge transformations: scalar, vector and tensor modes.
- Generation of gravitational waves during inflation.
- Second-order tensor modes. Linear evolution of GW. Upper bounds on the gravitational-wave background (GWB). Anisotropy and non-Gaussianity of the SGWB.

# The GW spectrum



# Second-order tensor modes and GW

Consider the spatial part of second-order Einstein equations and project them into their transverse and traceless parts:

$$\hat{\Pi}_{ij}^{lm} G_{lm}^{(2)} = \kappa^2 \hat{\Pi}_{ij}^{lm} T_{lm}^{(2)}$$

where  $\kappa^2 = 8\pi G$  and we introduced the tensor projector operator

$$\hat{\Pi}_{ij}^{lm} = \Pi_l^i \Pi_m^j - \frac{1}{2} \Pi_{ij} \Pi^{lm} \text{ with } \Pi_{ij} = \delta_{ij} - \partial_i \partial_j / \Delta$$

Consider the flat FLRW second-order perturbed metric, neglecting for simplicity first-order vector and tensor perturbations, and employ

$$h_{ij} \equiv h_{ij}^{(2)}.$$

# Notation

$$g_{00} = -a(\tau) \left( 1 + 2 \sum_{r=1}^{+\infty} \frac{1}{r!} \Psi^{(r)} \right),$$

$$g_{0i} = a^2(\tau) \sum_{r=1}^{+\infty} \frac{1}{r!} \omega_i^{(r)},$$

$$g_{ij} = a^2(\tau) \left\{ \left[ 1 - 2 \left( \sum_{r=1}^{+\infty} \frac{1}{r!} \Phi^{(r)} \right) \right] \delta_{ij} + \sum_{r=1}^{+\infty} \frac{1}{r!} h_{ij}^{(r)} \right\},$$

# Second-order tensor modes and GW

- From this expression the Einstein tensor at second-order results

$$G_j^{(2)i} = a^{-2} \left[ \frac{1}{4} (h_j''{}^i + 2\mathcal{H}h_j'^i - \nabla^2 h_j^i) + 2\Psi^{(1)} \partial^i \partial_j \Psi^{(1)} - 2\Phi^{(1)} \partial_i \partial_j \Psi^{(1)} \right. \\ \left. + 4\Phi^{(1)} \partial_i \partial_j \Phi^{(1)} + \partial^i \Psi^{(1)} \partial_j \Psi^{(1)} - \partial^i \Psi^{(1)} \partial_j \Phi^{(1)} - \partial^i \Phi^{(1)} \partial_j \Psi^{(1)} \right. \\ \left. + 3\partial^i \Phi^{(1)} \partial_j \Phi^{(1)} + \left( \Psi^{(2)}, \Psi^{(2)}, \omega_i^{(2)} \text{ term} \right) + (\text{diagonal part}) \delta_j^i \right].$$

- The stress-energy tensor fluid of our perfect can also be expanded up to second order

$$T_j^{(2)i} = \left( \rho^{(0)} + P^{(0)} \right) v^{(1)i} v_j^{(1)} + P^{(0)} \pi_j^{(2)i} + P^{(1)} \pi_j^{(1)i} + P^{(2)} \delta_j^i$$

# Second-order tensor modes and GW

- Using the expressions for the first-order perturbations of the energy-momentum tensor in terms of the linear metric perturbations and of the background value of the stress-energy tensor, we obtain

$$h''_{ij} + 2\mathcal{H}h'_{ij} - \nabla^2 h_{ij} = -4\hat{\Pi}_{ij}^{lm} \mathcal{S}_{lm},$$

$$\begin{aligned} \mathcal{S}_{lm} \equiv & 2\Psi\partial^l\partial_m\Psi - 2\Phi\partial^l\partial_m\Psi + 4\Phi\partial^l\partial_m\Phi + 4\Psi\partial^l\partial_m\Psi \\ & + \partial^l\Psi\partial_m\Psi - \partial^l\Psi\partial_m\Phi - \partial^l\Phi\partial_m\Psi + 3\partial^l\Phi\partial_m\Phi \\ & - \frac{4}{3(1+\omega)\mathcal{H}^2}\partial_l(\Phi' + 3\mathcal{H}\Psi)\partial_m(\Phi' + 3\mathcal{H}\Psi) \\ & - \frac{2c_S^2}{3\omega\mathcal{H}^2}[3\mathcal{H}(\mathcal{H}\Psi - \Phi') + \nabla^2\Phi]\partial_l\partial_m(\Psi - \Phi), \end{aligned}$$

$$\omega \equiv P^{(0)}/\rho^{(0)}, \quad \Psi \equiv \Psi^{(1)}, \quad \Phi \equiv \Phi^{(1)} \quad \text{and} \quad c_S = P^{(1)}/\rho^{(1)}$$

# Second-order tensor modes and GW

- To solve this equation it is convenient to Fourier-transform

$$h_{ij}(\mathbf{x}, \tau) = \int \frac{d^3\mathbf{k}}{(2\pi)^{3/2}} e^{i\mathbf{k}\cdot\mathbf{x}} [h_{\mathbf{k}}(\tau)\mathbf{e}_{ij}(\mathbf{k}) + \bar{h}_{\mathbf{k}}(\tau)\bar{\mathbf{e}}_{ij}(\mathbf{k})]$$

The two polarization tensors  $\mathbf{e}_{ij}$ ,  $\bar{\mathbf{e}}_{ij}$  can be expressed by the polarization vectors  $\mathbf{e}_i(\mathbf{k})$ ,  $\bar{\mathbf{e}}_i(\mathbf{k})$  orthogonal to the propagation vector  $\mathbf{k}$  as

$$(94) \quad \mathbf{e}_{ij}(\mathbf{k}) \equiv \frac{1}{\sqrt{2}} [\mathbf{e}_i(\mathbf{k})\mathbf{e}_j(\mathbf{k}) - \bar{\mathbf{e}}_i(\mathbf{k})\bar{\mathbf{e}}_j(\mathbf{k})],$$

$$(95) \quad \bar{\mathbf{e}}_{ij}(\mathbf{k}) \equiv \frac{1}{\sqrt{2}} [\mathbf{e}_i(\mathbf{k})\bar{\mathbf{e}}_j(\mathbf{k}) - \bar{\mathbf{e}}_i(\mathbf{k})\mathbf{e}_j(\mathbf{k})].$$

In terms of the polarization tensors, then the RHS of eq. (91) is written as

# Second-order tensor modes and GW

where  $\mathcal{S}_{lm}(\mathbf{k})$  is the Fourier transform of  $\mathcal{S}_{lm}(\mathbf{x}')$ . Then, the equation of motion of second-order tensor modes in Fourier space, for each polarization state, reads

$$h_{\mathbf{k}}'' + 2\mathcal{H}h_{\mathbf{k}}' + k^2 h_{\mathbf{k}} = \mathcal{S}(\mathbf{k}, \tau),$$

where the quantity

$$\mathcal{S}(\mathbf{k}, \tau) = -4e^{lm}(\mathbf{k})\mathcal{S}_{lm}(\mathbf{k})$$

is the convolution of two linear scalar perturbations. The equality (97) is a wave-equation with a source, whose solution reads

$$h_{\mathbf{k}}(\tau) = \frac{1}{a(\tau)} \int d\tilde{\tau} G_{\mathbf{k}}(\tau; \tilde{\tau}) [a(\tilde{\tau})\mathcal{S}(\mathbf{k}, \tilde{\tau})],$$

where the Green function  $G_{\mathbf{k}}$  solves the eq. (97) with the source given by  $(1/a)\delta(\tau - \tilde{\tau})$ .  $G_{\mathbf{k}}$  then depends only on the evolution of the scale-factor. Given eq. (99), the expression for the GW correlator can be written in terms of that of the source as

$$\begin{aligned} \langle h_{\mathbf{k}}(\tau)h_{\mathbf{k}'}(\tau) \rangle = \\ \frac{1}{a^2(\tau)} \int_{\tau_0}^{\tau} d\tilde{\tau}_1 d\tilde{\tau}_2 a(\tilde{\tau}_1) a(\tilde{\tau}_2) G_{\mathbf{k}}(\tau; \tilde{\tau}_1) G_{\mathbf{k}'}(\tau; \tilde{\tau}_2) \langle \mathcal{S}(\mathbf{k}, \tilde{\tau}_1) \mathcal{S}(\mathbf{k}', \tilde{\tau}_2) \rangle, \end{aligned}$$

where  $\tau_0$  is the time when the source switches on. Equation (100) represents the general expression for the GW power spectrum due to tensor modes that solve eq. (91). Then, now the interesting point is to find out the solution for specific cases of the source term.

# Second-order tensor modes sourced by inflaton fluctuations during inflation

The immediate application of second-order perturbation theory consists in considering the inflationary scalar perturbations as a source for GW. We have just seen that the very existence of scalar perturbations gives rise to tensor modes, independently of how the first-order scalars have been generated. Knowing the scalar power spectrum during the inflationary period, the sourced-GW power spectrum can be calculated too. The spectral properties of our scalar seeds are perfectly specified by

$$\langle \Phi_{\mathbf{k}} \Phi_{\mathbf{k}'} \rangle = \frac{2\pi^2}{k^3} P_{\Phi}(k) \delta(\mathbf{k} + \mathbf{k}')$$

We then have  $h_{\mathbf{k}}(\tau) = \frac{1}{a(\tau)} \int d\tilde{\tau} G_{\mathbf{k}}(\tau, \tilde{\tau}) [a(\tilde{\tau}) \mathcal{S}(\mathbf{k}, \tilde{\tau})]$  where the source (after extracting the polarization tensors) is convolved with the Green's function, which, in de Sitter space reads

$$G_{\mathbf{k}}(\tau, \tilde{\tau}) = \frac{1}{k^3 \tilde{\tau}^2} [(1 + k^2 \tau \tilde{\tau}) \sin k(\tau - \tilde{\tau}) + k(\tilde{\tau} - \tau) \cos k(\tau - \tilde{\tau})] \Theta(\tau - \tilde{\tau})$$

# Survey of GW generating mechanisms

Summary of the main mechanisms of GW production during inflation and the preheating phase. In the fourth column, the scenarios are reported as examples for each mentioned case (from Guzzetti et al. 2016).

| GW Production   | Discriminant      | Specific discriminant                 | Examples of specific models        | Produced GW           |
|---|-------------------|---------------------------------------|------------------------------------|-----------------------|
| Vacuum oscillations<br>quantum fluctuations of the gravitational field stretched by the accelerated expansion   | theory of gravity | General Relativity                    | <i>single-field slow-roll</i>      | <i>broad spectrum</i> |
|   |                   |                                       | all other models in GR             | broad spectrum        |
|   |                   | MG/EFT approach                       | G-Inflation                        | broad spectrum        |
|   |                   |                                       | Potential-driven G-Inflation       | broad spectrum        |
|   |                   |                                       | EFT approach                       | broad spectrum        |
| Classical production<br><br>second-order GW generated by the presence of a source term in GW equation of motion | source term       | vacuum inflaton fluctuations          | <i>all models</i>                  | <i>broad spectrum</i> |
|   |                   | fluctuations of extra scalar fields   | inflaton+spectator fields          | broad spectrum        |
|   |                   |                                       | curvaton                           | broad spectrum        |
|   |                   | gauge particle production             | pseudoscalar inflaton +gauge field | broad spectrum        |
|   |                   |                                       | scalar infl.+ pseudoscalar+gauge   | broad spectrum        |
|   |                   | scalar particle production            | scalar inflaton +scalar field      | peaked                |
|   |                   | particle production during preheating | chaotic inflation                  | peaked                |
| hybrid inflation  | peaked            |                                       |                                    |                       |

# Testing the Inflationary Consistency Relation

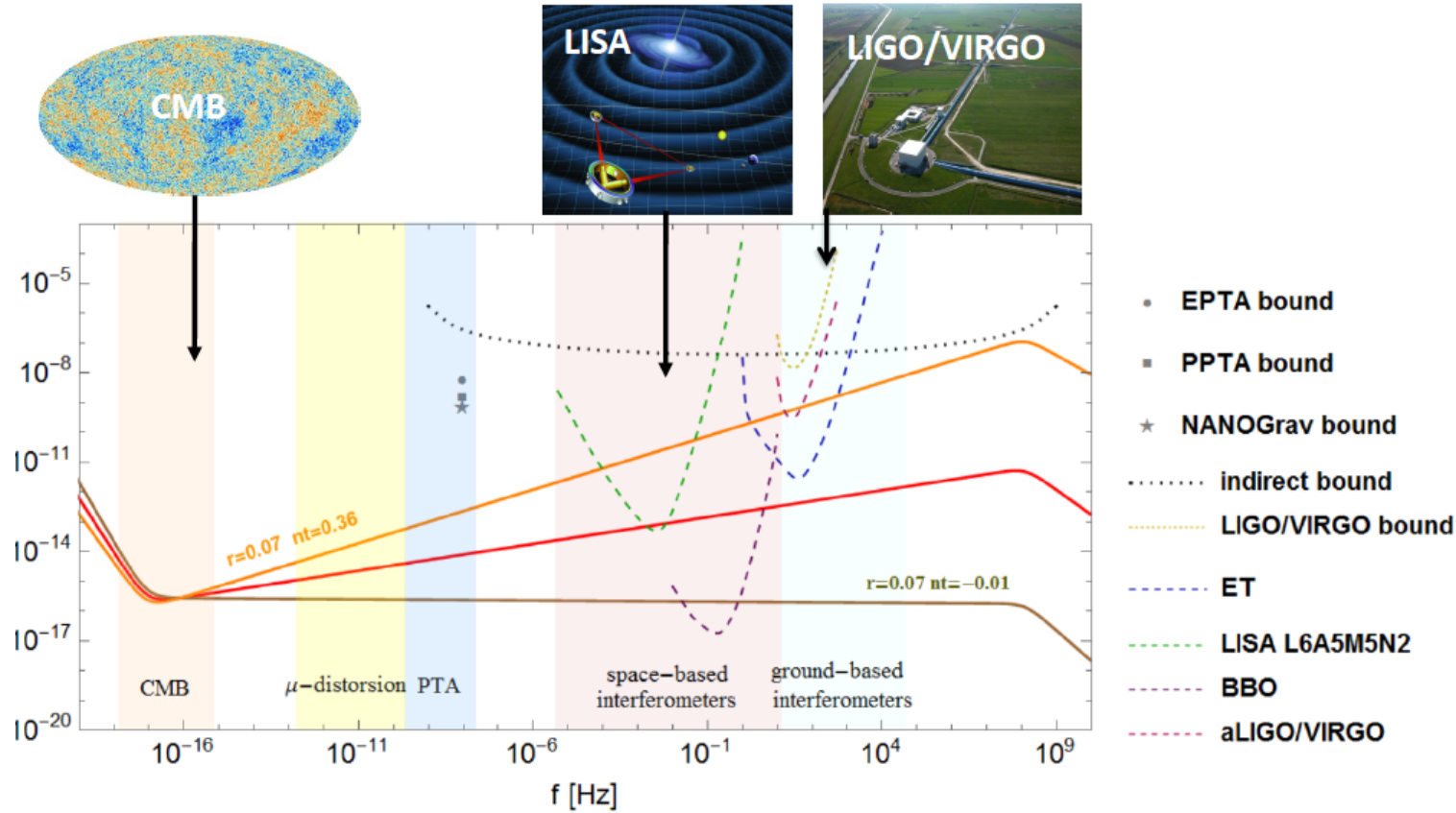
single-field slow-roll inflation  $r = -8n_T$

inflationary models beyond the standard ones  $\rightarrow$  violation

From Guzzetti, Bartolo, Liguori & Matarrese, "Gravitational waves from Inflation", 2016

|                  | Model                        | Tensor power-spectrum  | Tensor spectral index  |      | Consistency relation                 |
|------------------|------------------------------|--|--|------|--------------------------------------|
| Background       | Standard infl.               | $P_T = \frac{8}{M_{\text{pl}}^2} \left(\frac{H}{2\pi}\right)^2$  | $n_T = -2\epsilon$   | red  | $r = -8n_T$                          |
|                  | EFT inflation <sup>(a)</sup> | $P_T = \frac{8}{c_T M_{\text{pl}}^2} \left(\frac{H}{2\pi}\right)^2$  | $n_T = -2\epsilon + \frac{2}{3} \frac{m_T^2}{\alpha H^2} \left(1 + \frac{4}{3}\epsilon\right)$   | r/b  | -                                    |
|                  | EFT inflation <sup>(b)</sup> | $P_T = \frac{8}{c_T M_{\text{pl}}^2} \frac{2^{-p}}{\pi} \Gamma^2\left(\frac{1}{2(1+p)}\right) \left(\frac{H}{2\pi}\right)^2$ | $n_T = \frac{p}{1+p}$  | blue | violation                            |
|                  | Gen. G-Infl.                 | $P_T = \frac{8}{M_{\text{pl}}^2} \gamma_T \frac{\mathcal{G}_T^{1/2}}{\mathcal{F}_T^{3/2}} \left(\frac{H}{2\pi}\right)^2$     | $n_T = 3 - 2\nu_T$   | r/b  | -                                    |
|                  | Pot.-driv. G-Infl.           | $P_T = \frac{8}{M_{\text{pl}}^2} \left(\frac{H}{2\pi}\right)^2$  | $n_T = -2\epsilon$   | r/b  | $r \simeq -\frac{32\sqrt{6}}{9} n_T$ |
| Extra background | Particle prod.               | $P_T^+ = 8.6 \times 10^{-7} \frac{4H^2}{M_{\text{pl}}^2} \left(\frac{H}{2\pi}\right)^2 \frac{e^{4\pi\epsilon}}{\xi^6}$       | -  | blue | violation                            |
|                  | Spectator field              | $P_T \simeq 3 \frac{H^4}{c_S^{18/5} M_{\text{pl}}^4}$  | $n_T \simeq 2 \left(\frac{2m^2}{3H^2} - 2\epsilon\right) - \frac{18}{5} \frac{\dot{c}_S}{H c_S}$ | r/b  | violation                            |

From: Guzzetti, Bartolo., Liguori, Matarrese, "Gravitational waves from Inflation" 2016



Target of future CMB experiments:  $r < 10^{-3}$

# Prospects for PGWB detection

Capurri, Bartolo, Maino and Matarrese (2020, in preparation) study EFT models producing blue GW spectra

# Gauge dependence of second-order tensor modes

- Matarrese, Mollerach & Bruni (1998) computed second-order tensor modes in two gauges in matter-dominant: synchronous-comoving (S) and Poisson (P) gauges, finding extra (non-oscillatory) terms in the S-gauge.

- S-gauge

$$\mathcal{S}_{ij} = \nabla^2 \Psi_0 \delta_{ij} + \Psi_{0,ij} + 2(\varphi_{,ij} \nabla^2 \varphi - \varphi_{,ik} \varphi_{,j}{}^{,k})$$

$$\pi''_{Sij} + \frac{4}{\tau} \pi'_{Sij} - \nabla^2 \pi_{Sij} = -\frac{\tau^4}{21} \nabla^2 \mathcal{S}_{ij}$$

$$\nabla^2 \Psi_0 = -\frac{1}{2} [(\nabla^2 \varphi)^2 - \varphi_{,ik} \varphi^{,ik}]$$

- which is solved by

$$\pi_{ij}(\mathbf{x}, \tau) = \frac{\tau^4}{21} \mathcal{S}_{ij}(\mathbf{x}) + \frac{4\tau^2}{3} \mathcal{T}_{ij}(\mathbf{x}) + \tilde{\pi}_{ij}(\mathbf{x}, \tau)$$

$$\nabla^2 \mathcal{T}_{ij} = \mathcal{S}_{ij}$$

$$\tilde{\pi}_{ij}(\mathbf{x}, \tau) = \frac{1}{(2\pi)^3} \int d^3\mathbf{k} \exp(i\mathbf{k} \cdot \mathbf{x}) \frac{40}{k^4} \mathcal{S}_{ij}(\mathbf{k}) \left( \frac{1}{3} - \frac{j_1(k\tau)}{k\tau} \right)$$

# Gauge dependence of second-order tensor modes

- In the P-gauge one only gets

$$\tilde{\pi}_{ij}'' + \frac{4}{\tau} \tilde{\pi}_{ij}' - \nabla^2 \tilde{\pi}_{ij} = -\frac{40}{3} \mathcal{T}_{ij}$$

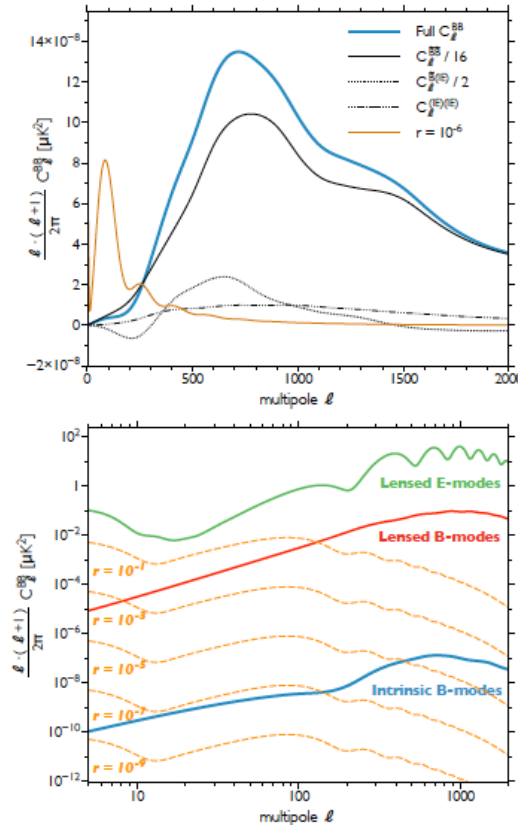
which is solved by our previous expression

$$\tilde{\pi}_{ij}(\mathbf{x}, \tau) = \frac{1}{(2\pi)^3} \int d^3\mathbf{k} \exp(i\mathbf{k}\cdot\mathbf{x}) \frac{40}{k^4} \mathcal{S}_{ij}(\mathbf{k}) \left( \frac{1}{3} - \frac{j_1(k\tau)}{k\tau} \right)$$

- Inomata & Terada (2019) have shown that the same result is found in the TT gauge (contrary to previous claims). They conclude that the “gravitational-wave” part is indeed gauge-independent, while extra non-oscillatory terms of the second-order tensor modes may indeed differ from gauge to gauge. See also Yuan et al. (2019) and Gong (2020)

# Scalar-induced second-order (vector) and tensor modes produce CMB B-mode polarization

- Mollerach, Harari & Matarrese (2004) showed that a nonvanishing  $B$ -mode polarization unavoidably arises from pure scalar initial perturbations, thus limiting our ability to detect the signature of primordial gravitational waves generated during inflation. This secondary effect dominates over that of primordial tensors for an inflationary tensor-to-scalar ratio  $r < 10^{-6}$ . The magnitude of the effect is smaller than the contamination produced by the conversion of polarization of type  $E$  into type  $B$ , by weak gravitational lensing. However, the lensing signal can be cleaned, making the secondary modes discussed here the actual background limiting the detection of small amplitude primordial gravitational wave.
- A more refined analytical calculation was performed by Fidler et al. (2014)



from Fidler et al. (2014)

**Figure 1.** Angular power spectrum  $C_\ell^{BB}$  of the intrinsic B-polarisation in the CMB. In this and in the following figures, we show the  $C_\ell$ 's multiplied by a factor  $T_{\text{cmb}}^2 = (2.7255 \times 10^6 \mu\text{K})^2$  with respect to the equations in the text. *Upper panel:* breakdown of the intrinsic signal (solid blue curve) into its components, according to eq. (4.5). The  $BB$  contribution (solid) dominates over the quadratic contributions  $\bar{B}(IE)$  (dotted) and  $(IE)(IE)$  (dot-dashed), due to the partial cancellation between the redshift and temperature corrections eq. (3.13), as explained in the text. *Lower panel:* the intrinsic signal (solid blue curve) is comparable to that from primordial gravitational waves (dashed orange curves) with  $r \approx 10^{-7}$  at  $\ell = 100$  and  $r \approx 5 \times 10^{-5}$  at  $\ell \approx 700$ . It is always subdominant with respect to the lensing-induced B-modes (red curve) and the E-modes (green curve).

# Post-inflationary evolution of GW

Let us have a look at how GW behave at the time of radiation and matter domination, when accelerated expansion has already ended. Inflation stretches tensor perturbations wavelengths to super-horizon scales, making their amplitude almost frozen. During the radiation and subsequent matter eras, tensor perturbation wavelengths re-enter the horizon sequentially. When this happens the decaying solution has substantially disappeared, so what re-enters the causally connected space is the almost scale-invariant power spectrum at the time of first horizon crossing, which occurred during inflation. Then, modes that are inside the horizon, start oscillating with amplitude damped by a factor  $1/a$ . In particular, the GW field equation becomes a Bessel equation with the following solutions respectively, in terms of  $h_{k,i}$  modes:

$$h_k(\tau) = h_{k,i} j_0(k\tau), \quad h_k(\tau) = h_{k,i} \left( \frac{3j_1(k\tau)}{k\tau} \right),$$

radiation era                      matter era

where  $h_{k,i}$  is the amplitude at horizon crossing and  $j_0$  and  $j_1$  are the Bessel functions. Looking at the dependence on  $k$ , these solutions tell us that tensor perturbations start oscillating with a damping factor greater for high frequency waves. During an era of pure dominance of the cosmological constant, the space-time assumes a de Sitter metric so that the scale-factor evolves in an exponential way, as during inflation in case of  $\epsilon = 0$ . Then, in such an epoch, the form of the solution of the GW equation of motion is given by the standard inflationary solution.

# Damping of GW by cosmic neutrinos

Weinberg (2004) showed that the free-streaming of cosmic neutrinos (i.e. after their decoupling) produces a traceless transverse part of the anisotropic stress tensor which affects the propagation of cosmological gravitational waves, reducing their squared amplitude by 35.6% for wavelengths that enter the horizon during the radiation-dominated phase, independent of any cosmological parameters. This decreases the tensor temperature and polarization correlation functions for these wavelengths by the same amount. The effect is less for wavelengths that enter the horizon at later times. At the longest wavelengths the decrease in the tensor correlation functions due to neutrino free streaming being about 10%.

Consider the GW equation

$$\ddot{h}_{ij} + \left(\frac{3\dot{a}}{a}\right)\dot{h}_{ij} - \left(\frac{\nabla^2}{a^2}\right)h_{ij} = 16\pi G \pi_{ij}$$

The neutrino stress-energy tensor contains their phase-space distribution which is a solution of the Boltzmann equation in a perturbed FLRW universe. GW contribute to these perturbations and therefore affect the neutrino anisotropic stress

$$h''_{ij}(u) + \frac{2a'(u)}{a(u)}h'_{ij}(u) + h_{ij}(u) = -24f_\nu(u)\left(\frac{a'(u)}{a(u)}\right)^2 \int_0^u K(u-U)h'_{ij}(U)dU,$$

where  $u \equiv k \int_{t_1}^t \frac{dt'}{a(t')}$  and  $f_\nu \equiv \bar{\rho}_\nu / \bar{\rho}$  is the mean neutrino contribution to the energy density.

# GW as extra-radiation (modes well inside the horizon)

The energy density of a GW background decays with the expansion of the universe as relativistic degrees of freedom, i.e.  $\rho_{\text{GW}} \propto a^{-4}$ . This means that a GW background acts as an additional radiation field in the universe, contributing to the background expansion rate as

$$H^2(a) = H_0^2 \left[ \left( \frac{\rho_{\text{GW}}^0}{\rho_c^0} + \Omega_{\text{rad}}^0 \right) \left( \frac{a_0}{a} \right)^4 + \Omega_{\text{mat}}^0 \left( \frac{a_0}{a} \right)^3 + \Omega_{\Lambda}^0 \right]$$

We can then give a constraint on the GW energy density redshifted up to the present number in terms of the number of extra neutrino species

$$\left( \frac{h^2 \rho_{\text{GW}}}{\rho_c} \right)_0 \leq h^2 \Omega_{\gamma}^0 \left( \frac{g_S(T_0)}{g_S(T)} \right)^{4/3} \frac{7}{8} \Delta N_{\nu} = 5.6 \times 10^{-6} \Delta N_{\nu} \sim 10\%$$

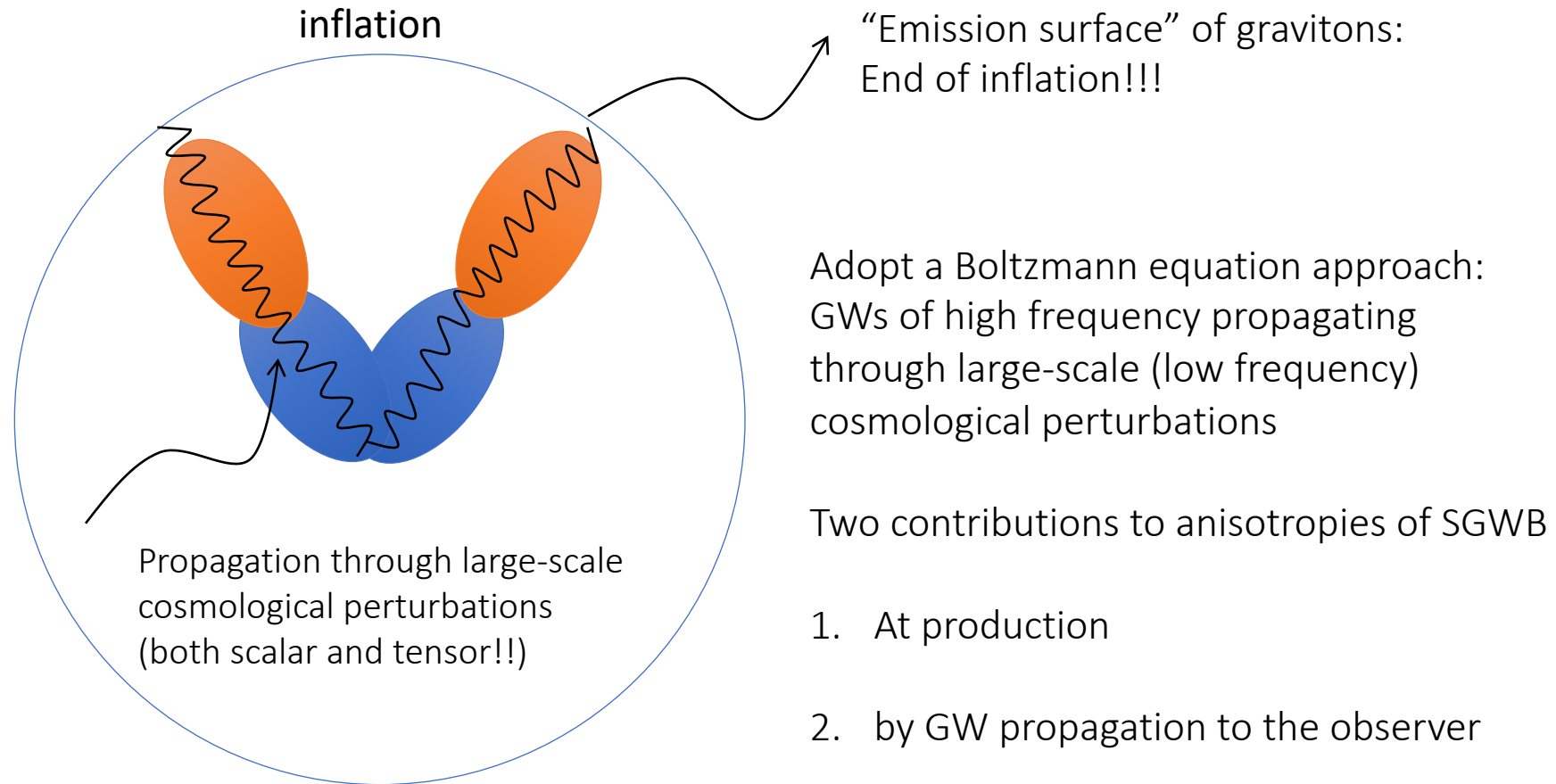
# Bibliography

- Based on:
- N. Bartolo, D. Bertacca, S. Matarrese, M. Peloso, A. Ricciardone, A. Riotto & G. Tasinato “Anisotropies and non-Gaussianity of the Cosmological Gravitational Wave Background”, Phys. Rev. D100 121501 (2019) [arXiv:1908.00527]
- N. Bartolo, D. Bertacca, S. Matarrese, M. Peloso, A. Ricciardone, A. Riotto & G. Tasinato, “Characterizing the Cosmological Gravitational Wave Background Anisotropies and non-Gaussianity,” arXiv:1912.09433
- For previous work see:
- V. Alba & J. Maldacena “Primordial gravity wave background anisotropies,” JHEP 1603, 115 (2016) [arXiv:1512.01531].
- C.R. Contaldi, “Anisotropies of Gravitational Wave Backgrounds: A Line Of Sight Approach”, Phys. Lett. B 771, 9 (2017) [arXiv:1609.08168].

# Cosmological SGWB anisotropies

- A derivation of the angular power spectrum of cosmological anisotropies, using a Boltzmann approach, has been obtained in [Alba & Maldacena 2016 (1512.01531), Contaldi 2017 (1609.08168) , Bartolo et al 2019 (1908.00527)] Bartolo et al. 2019b; 2019c
- Anisotropies in the cosmological background are imprinted both at its production and by GW propagation through the large-scale scalar and tensor perturbations of the universe. Note that the first contribution is not present in the CMB radiation (as the universe is not transparent to photons before recombination), causing an order one dependence of the anisotropies on frequency.
- We provided a new method to characterize the cosmological SGWB through its possible deviation from a Gaussian statistics. In particular, the SGWB will become a new probe of the primordial non-Gaussianity of the large-scale cosmological perturbations.

# Anisotropies of SGWB from inflation



The SGWB also brings frequency information, in contrast with CMB (apart from spectral distortions)

# Anisotropies of SGWB from inflation

Boltzmann equation approach

$$\underbrace{\frac{\partial f}{\partial \eta} + n^i \frac{\partial f}{\partial x^i}}_{\text{Free streaming: keeps memory of initial conditions!!!}} + \underbrace{\left[ \frac{\partial \Psi}{\partial \eta} - n^i \frac{\partial \Phi}{\partial x^i} + \frac{1}{2} n^i n^j \frac{\partial h_{ij}}{\partial \eta} \right]}_{\text{Gravitational effects that imprint anisotropies during propagation}} q \frac{\partial f}{\partial q} = 0 \quad (3)$$

Free streaming:  
keeps memory of initial  
conditions!!!

Gravitational effects that imprint anisotropies during propagation

$$\delta f \equiv -q \frac{\partial \bar{f}}{\partial q} \Gamma(\eta, \vec{x}, q, \hat{n}) \quad \text{In the case of CMB}$$

$$\Gamma_{\text{CMB}} = \delta T/T$$

$$\delta_{\text{GW}} = \underbrace{\left[ 4 - \frac{\partial \ln \bar{\Omega}_{\text{GW}}(\eta, q)}{\partial \ln q} \right]}_{\text{fixed by Planck distribution in the case of the CMB}} \Gamma(\eta, \vec{x}, q, \hat{n})$$

fixed by Planck distribution in the case of the CMB

Credits: N. Bartolo

# Anisotropies of the SGWB from inflation

$$\Gamma_I = e^{ik\mu(\eta_{\text{in}} - \eta)} \Gamma(\eta_{\text{in}}, \vec{k}, q, \hat{n})$$

Anisotropies at production:  
O(1)-dependence on frequency  $q$

$$\begin{aligned} \Gamma(\eta, \vec{k}, q, \hat{n}) = & \int_{\eta_{\text{in}}}^{\eta} d\eta' e^{ik\mu(\eta' - \eta)} \left\{ \Gamma(\eta', \vec{k}, q, \hat{n}) \delta(\eta' - \eta_{\text{in}}) \right. \\ & \left. + \Phi(\eta', \vec{k}) \delta(\eta' - \eta_{\text{in}}) + \frac{\partial [\Psi(\eta', \vec{k}) + \Phi(\eta', \vec{k})]}{\partial \eta'} \left[ \frac{1}{2} n_i n_j \frac{\partial h_{ij}(\eta', \vec{k})}{\partial \eta'} \right] \right\} \end{aligned}$$

Anisotropies from propagation through scalar perturbations

Anisotropies from propagation through tensor perturbations

$$\Gamma(\hat{n}) = \sum_{\ell} \sum_{m=-\ell}^{\ell} \Gamma_{\ell m} Y_{\ell m}(\hat{n}) \longrightarrow \Gamma_{\ell m} = \Gamma_{\ell m, I}(q) + \Gamma_{\ell m, S} + \Gamma_{\ell m, T}$$

$$\Gamma_{\ell m} \sim \int d^3 k X \mathcal{T}_{\ell}^{(X)}(k, \eta_0, \eta_{\text{in}})$$

Seed: can be  $\Gamma_I(\eta_{\text{in}}, k, q)$ ,  $\zeta$  or  $h_{ij}$

Transfer function

Credits: N. Bartolo

# Frequency dependence of initial anisotropies

$$\Gamma(\eta_0, \vec{x}_0, q, \hat{n}) = \Gamma_I(\eta_0, \vec{x}_0, q, \hat{n}) + \Gamma_S(\eta_0, \vec{x}_0, \hat{n}) + \Gamma_T(\eta_0, \vec{x}_0, \hat{n})$$

What about initial conditions?

What about their frequency dependence?

- This contribution is completely erased by collisions in the case of CMB anisotropies (and frequency dependence in CMB arises only at second-order in the perturbations).
- Instead for the case of a primordial SGWB visible at interferometers scales this term is present and can lead to anisotropies with large (order-one) frequency dependence.

# Non-Gaussianity in SGB anisotropies

Induced by:

- Initial conditions (e.g. in PBH models)
- Propagation through non-Gaussian scalar modes
- Propagation through non-Gaussian tensor modes (e.g. as those arising from second-order scalar modes, as originally proposed by K. Tomita (1967); Matarrese & Mollerach 1997, ... → note that also tensor modes generate GW at second order; Matarrese, Mollerach & Bruni 1998; Mollerach, Harari & Matarrese 2004).
- Use Weinberg theorem for adiabatic modes to study NG in squeezed limit avoiding *potential* gauge artifacts.

# “Standard” PNG model

Many primordial (inflationary) models of non-Gaussianity can be represented in configuration space by the simple formula (Salopek & Bond 1990; Gangui et al. 1994; Verde et al. 1999; Komatsu & Spergel 2001)

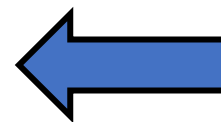
$$\Phi = \phi_L + f_{\text{NL}} * (\phi_L^2 - \langle \phi_L^2 \rangle) + g_{\text{NL}} * (\phi_L^3 - \langle \phi_L^2 \rangle \phi_L) + \dots$$

where  $\Phi$  is the large-scale gravitational potential (more precisely  $\Phi = 3/5 \zeta$  on superhorizon scales, where  $\zeta$  is the gauge-invariant comoving curvature perturbation),  $\phi_L$  its linear Gaussian contribution and  $f_{\text{NL}}$  the dimensionless *non-linearity parameter* (or more generally *non-linearity function*). The percent of non-Gaussianity in CMB data implied by this model is

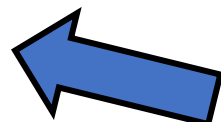
$$\text{NG \%} \sim 10^{-5} |f_{\text{NL}}|$$

$$\sim 10^{-10} |g_{\text{NL}}|$$

“non-Gaussian = non-dog”  
(Ya.B. Zel’dovich)



< 10<sup>-5</sup> from  
CMB & LSS



< 10<sup>-5</sup> from  
CMB & LSS

# Bispectrum & PNG: theoretical expectations

- Primordial NG probed fundamental physics during inflation, being sensitive to *(self-)interactions* of fields present during inflation (different inflationary models predict different *amplitudes and shapes* of the bispectrum)
- Standard models of slow-roll inflation predict only a *tiny deviation from Gaussianity* (Salopek & Bond '90; Gangui, Lucchin, Matarrese & Mollerach 1995; Acquaviva, Bartolo, Matarrese & Riotto 2003; Maldacena 2003), arising from *non-linear gravitational interactions* during inflation. See, Matarrese, Pilo & Rollo (in preparation), for a discussion of the observability of Maldacena's consistency relation.

*Planck results are fully consistent with such a prediction!*

- PNG probes interactions among particles at inflation energy scales. See literature on probing string-theory via oscillatory PNG (Arkani-Hamed & Maldacena 2015 "Cosmological collider physics"; Silverstein 2017 "The dangerous irrelevance of string theory").

# *Planck* 2018 results IX: *Planck* collaboration 2019

PNG Planck project (Coordinators: S. Matarrese & B. Wandelt)

- Constrain (with high precision) and/or detect primordial non-Gaussianity (NG) as due to (non-standard) inflation
- We tested: *local*, *equilateral*, *orthogonal* shapes (+ many more) for the bispectrum and constrain primordial trispectrum parameter  $g_{\text{NL}}$  ( $\tau_{\text{NL}}$  constrained in previous release).
- We have completed the final, *Planck* legacy release, which improves the 2015 results in terms of more refined treatment of E-mode polarization (including low- $l$  region).

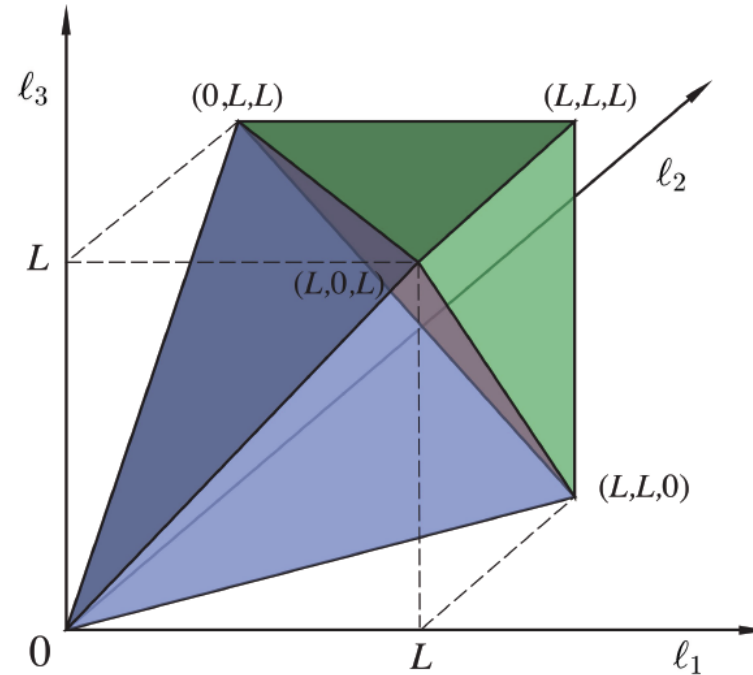
# CMB bispectrum representation

$$B_{\ell_1 \ell_2 \ell_3}^{m_1 m_2 m_3} \equiv \langle a_{\ell_1 m_1} a_{\ell_2 m_2} a_{\ell_3 m_3} \rangle$$

$$= \mathcal{G}_{m_1 m_2 m_3}^{\ell_1 \ell_2 \ell_3} b_{\ell_1 \ell_2 \ell_3}$$

Gaunt integrals

$$\begin{aligned} \mathcal{G}_{m_1 m_2 m_3}^{\ell_1 \ell_2 \ell_3} &\equiv \int Y_{\ell_1 m_1}(\hat{\mathbf{n}}) Y_{\ell_2 m_2}(\hat{\mathbf{n}}) Y_{\ell_3 m_3}(\hat{\mathbf{n}}) d^2 \hat{\mathbf{n}} \\ &= h_{\ell_1 \ell_2 \ell_3} \begin{pmatrix} \ell_1 & \ell_2 & \ell_3 \\ m_1 & m_2 & m_3 \end{pmatrix}, \end{aligned}$$

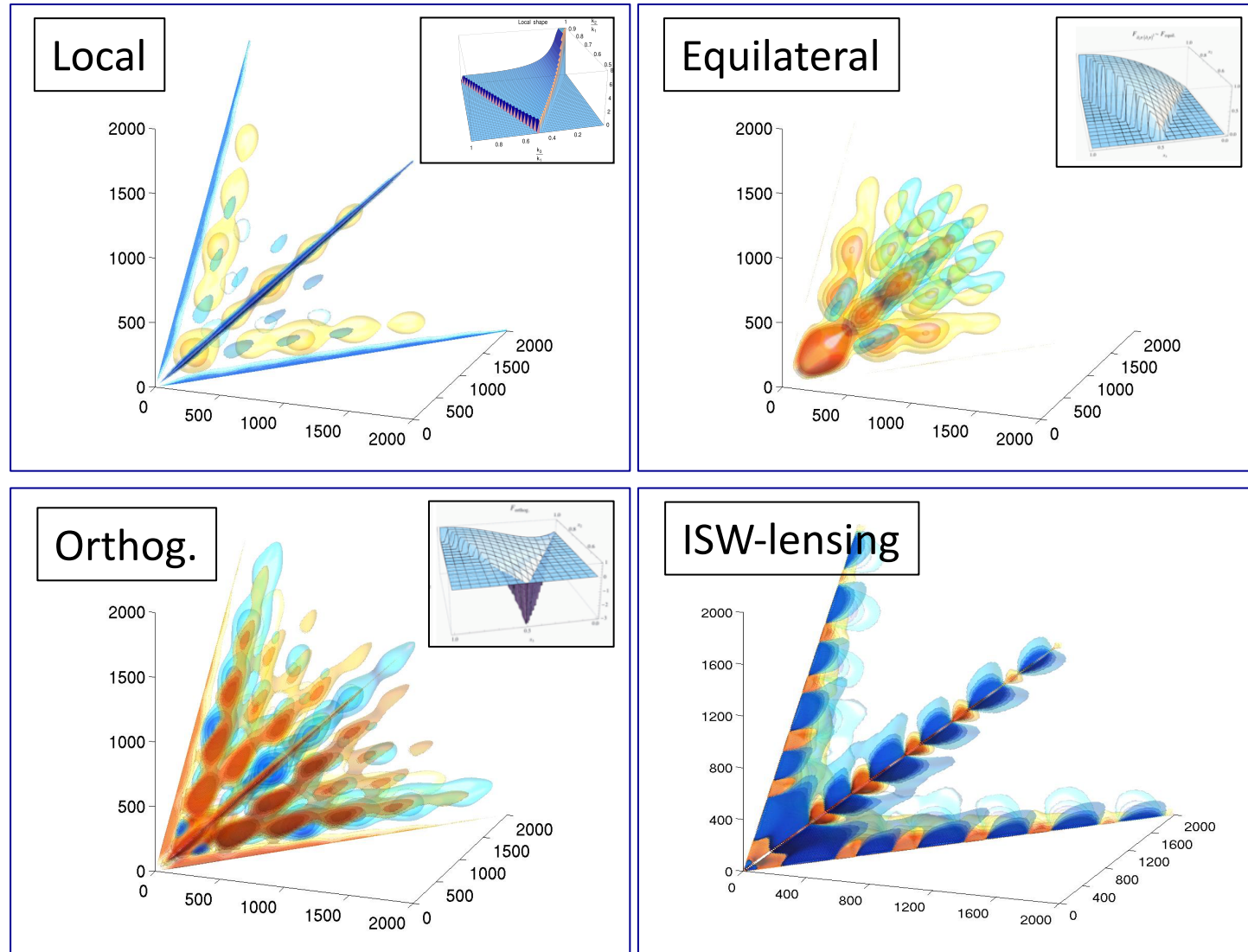


Triangle condition:  $\ell_1 \leq \ell_2 + \ell_3$  for  $\ell_1 \geq \ell_2, \ell_3$ , +perms.

Parity condition:  $\ell_1 + \ell_2 + \ell_3 = 2n$ ,  $n \in \mathbb{N}$ ,

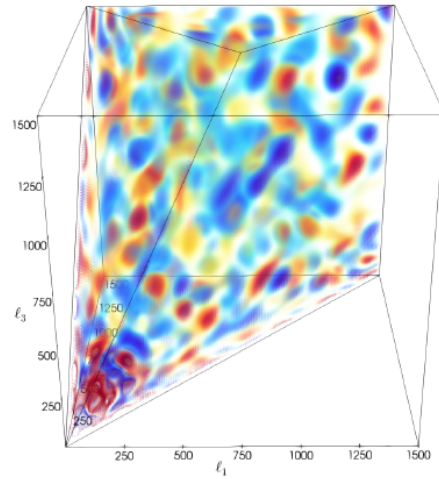
Resolution:  $\ell_1, \ell_2, \ell_3 \leq \ell_{\max}$ ,  $\ell_1, \ell_2, \ell_3 \in \mathbb{N}$ .

# Bispectrum shapes (modal representation)

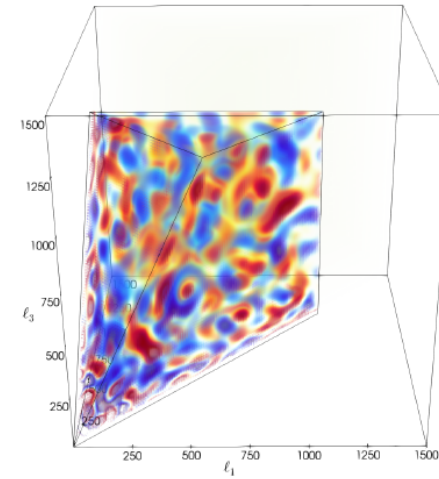


# The *Planck* bispectrum (modal; 2018)

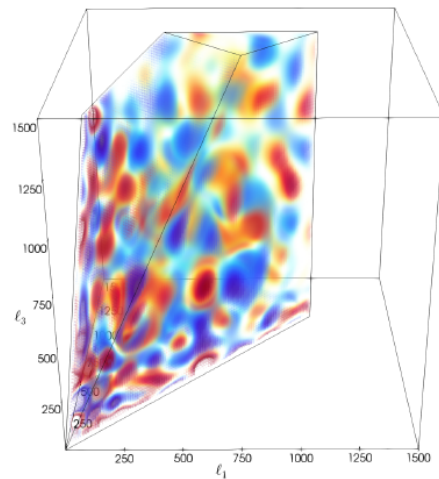
**TTT**



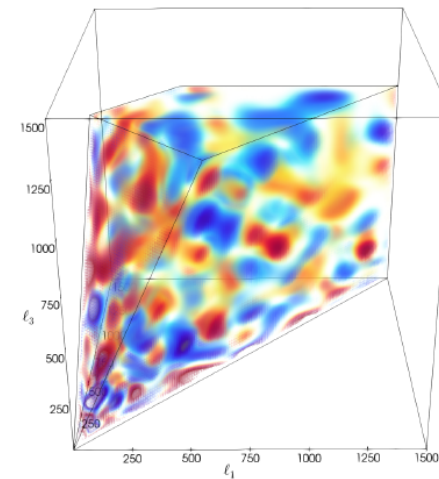
**EEE**



**TTE**



**EET**



(S/N  
weighted)

# $f_{\text{NL}}$ from *Planck* 2018 bispectrum (KSW)

| Shape                 | Independent      | Lensing subtracted |
|-----------------------|------------------|--------------------|
|                       | SMICA <i>T</i>   |                    |
| Local . . . . .       | $6.7 \pm 5.6$    | $-0.5 \pm 5.6$     |
| Equilateral . . . . . | $4 \pm 67$       | $5 \pm 67$         |
| Orthogonal . . . . .  | $-38 \pm 37$     | $-15 \pm 37$       |
|                       | SMICA <i>T+E</i> |                    |
| Local . . . . .       | $4.1 \pm 5.1$    | $-0.9 \pm 5.1$     |
| Equilateral . . . . . | $-25 \pm 47$     | $-26 \pm 47$       |
| Orthogonal . . . . .  | $-47 \pm 24$     | $-38 \pm 24$       |

# CMB constraints on tensor PNG

**Table 14.** Results for the tensor nonlinearity parameter  $f_{\text{NL}}^{\text{tens}}/10^2$  obtained from the SMICA, SEVEM, NILC, and Commander temperature and polarization maps. The central values and the errors (68 % CL) extracted from  $\ell_1 + \ell_2 + \ell_3 = \text{even}$  (“Even”),  $\ell_1 + \ell_2 + \ell_3 = \text{odd}$  (“Odd”), and their whole domain (“All”) are separately described. One can see that all  $T$ -only results are in good agreement with both the *Planck* 2015 ones (PCNG15) and WMAP ones (Shiraishi et al. 2015).

|                  | Even         | Odd             | All          |
|------------------|--------------|-----------------|--------------|
| <b>SMICA</b>     |              |                 |              |
| $T$ .....        | $4 \pm 17$   | $100 \pm 100$   | $6 \pm 16$   |
| $E$ .....        | $33 \pm 67$  | $-570 \pm 720$  | $29 \pm 67$  |
| $T+E$ .....      | $11 \pm 14$  | $1 \pm 18$      | $8 \pm 11$   |
| <b>SEVEM</b>     |              |                 |              |
| $T$ .....        | $4 \pm 17$   | $90 \pm 100$    | $6 \pm 16$   |
| $E$ .....        | $75 \pm 75$  | $-790 \pm 830$  | $70 \pm 75$  |
| $T+E$ .....      | $16 \pm 14$  | $2 \pm 20$      | $13 \pm 12$  |
| <b>NILC</b>      |              |                 |              |
| $T$ .....        | $4 \pm 17$   | $90 \pm 100$    | $6 \pm 16$   |
| $E$ .....        | $-16 \pm 81$ | $-540 \pm 820$  | $-19 \pm 80$ |
| $T+E$ .....      | $6 \pm 14$   | $3 \pm 21$      | $5 \pm 11$   |
| <b>Commander</b> |              |                 |              |
| $T$ .....        | $5 \pm 17$   | $90 \pm 100$    | $6 \pm 16$   |
| $E$ .....        | $21 \pm 69$  | $-1200 \pm 700$ | $13 \pm 69$  |
| $T+E$ .....      | $10 \pm 14$  | $-2 \pm 19$     | $7 \pm 11$   |

# PNG and precision cosmology

- PNG is currently the highest precision test of Standard Inflation models.
- With Planck:
  - PNG constrained at better than  $\sim 0.01\%$
  - Flatness constrained at  $\sim 0.1\%$
  - Isocurvature mode constrained at  $\sim 1\%$

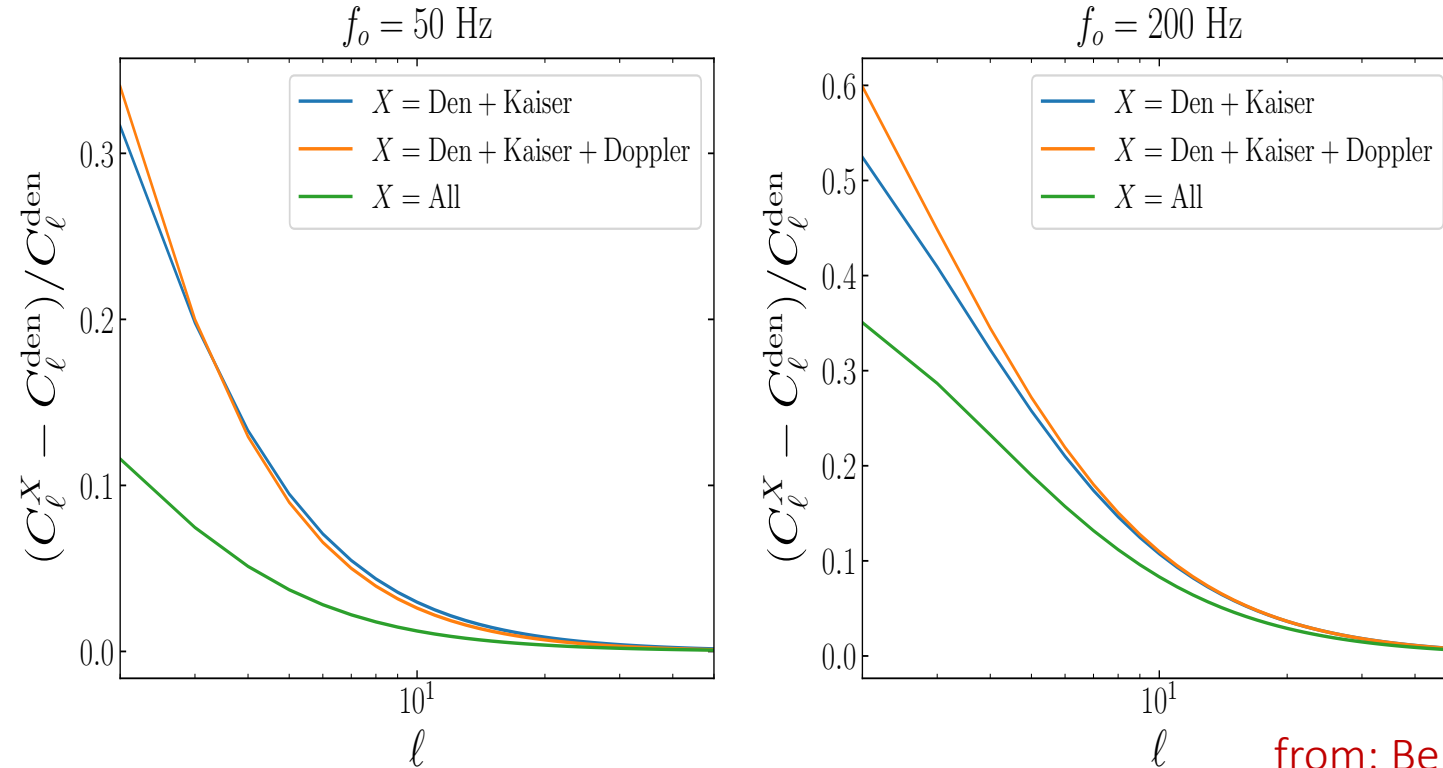
# Astrophysical Stochastic Gravitational-Wave Background (ASGWB)

- A gravitational wave stochastic background of astrophysical origin may result from the **superposition of a large number of unresolved sources since the beginning of stellar activity.**
- Its detection would put very strong **constraints on the physical properties of compact objects, the initial mass function or the star formation history.**
- Qualitatively one expects that the ASGWB will be dominated by sources typically 3–4 orders of magnitude fainter in luminosity than sources in relatively nearby galaxies at 10–100 Mpc ( $z \approx 0.002$ – $0.02$ ).

# ASGWB anisotropies

- Angular power-spectrum obtained by Cusin et al. (2017, 2018a,b), considering the presence of inhomogeneities in the matter distribution and working with a coarse-graining approach, which allow to probe GW sources on cosmological, galactic and sub-galactic scales.
- Predictions for the GW angular power spectrum have been derived by Jenkins et al (2018a,b), where both analytical expression and numerical studies, using a mock galaxy catalogue from Millennium simulation, are presented.
- Bertacca et al. (2019) accounted for all projection effects, adopting the cosmic rulers formalism and gauge-invariant variables, as done for galaxy surveys, finding results fully analogous to those obtained for other cosmic backgrounds from unresolved sources (e.g. CIB analysis by Desjacques et al. 2019). Alternative approach presented by Pitrou et al. (2019).

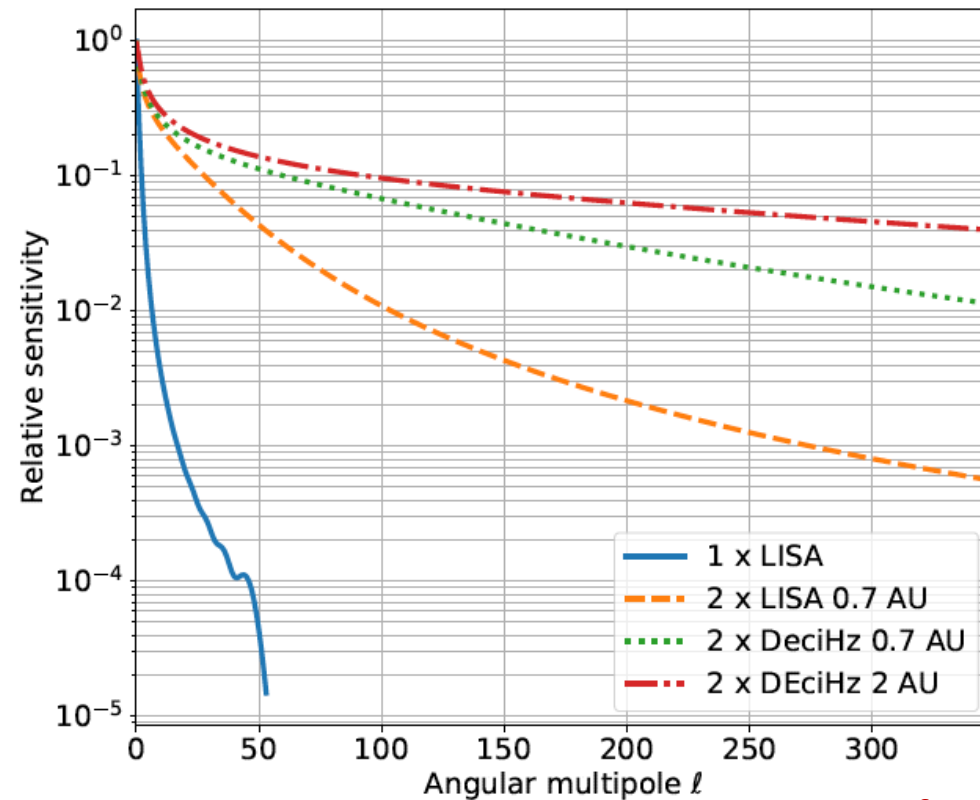
# SGWB generated by black-hole mergers in the frequency range of LIGO-Virgo



from: Bertacca et al. 2019

Only **unresolved sources contribute to the SGWB**. We consider GWs emission in  $f_o = 50$  Hz and  $f_o = 200$  Hz channels, assuming that all black-hole binaries have members with masses  $(\text{MBH}_1, \text{MBH}_2) = (15 M_\odot, 15 M_\odot)$  and zero spin. For simplicity, we assume here that all the events come from halos with mass  $M_h = 10^{12} M_\odot$ .

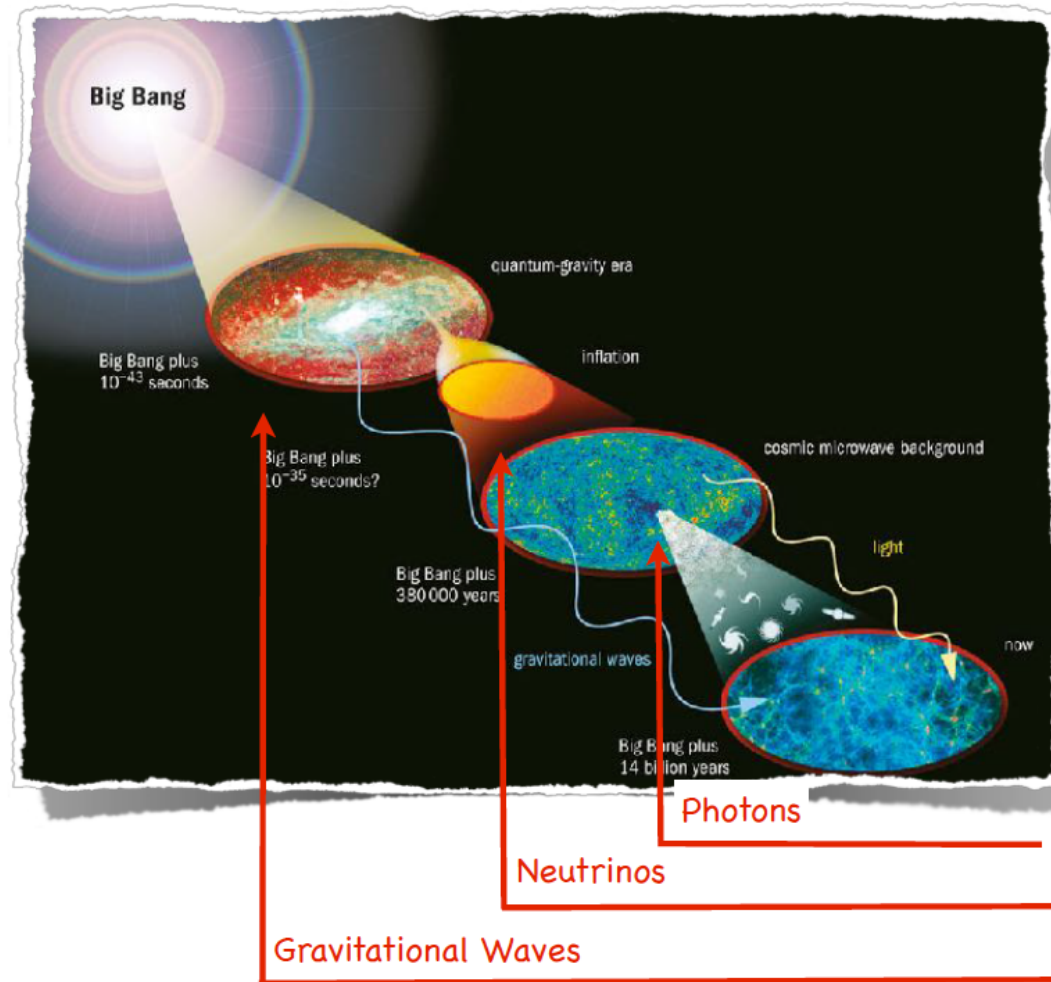
# Angular resolution of GW detectors



from: Baker et al. 2019

Idealized angular resolution for different detector configurations (see text). The relative sensitivity to different angular multipoles is obtained by integrating the spherical response to a cross-correlation baseline weighted by a simple model of the noise spectrum based on the individual detector arm lengths. Convolution with the detector response functions and the sky-phase coverage would give additional structure on top of the idealized case.

# GW carry information on the earliest epochs in the cosmic history



Primordial GWs are out of equilibrium since the Planck scale (photons at 0.3 eV) so they carry information about the Universe at really high energies

# Final remarks on Part III

- GW carry information on the earliest epochs of the cosmic history → anisotropies of the GWB represent a snapshot the Universe at GW decoupling/GW production at horizon exit during inflation
- Unlike the CMB, the GWB is non-thermal, hence its frequency spectrum is also representative of the physical processes occurring at those very early epochs.
- Presently SGWB anisotropies are likely to be dominated by the background produced by unresolved astrophysical sources, which has to be studied in great detail. Is the latter Gaussian, as commonly claimed?

# Concluding remarks: the next challenge

- Inflation provides a causal mechanism for the generation of cosmological perturbations
- CMB and LSS data fully support the detailed predictions of inflation
- The direct detection of:
  - Primordial Gravitational-Wave Background
  - Primordial non-Gaussianity

with the specific features predicted by inflation would provide strong independent support to the model.